Biomedical Microdevices (2018) 20: 32
https://doi.org/10.1007/s10544-018-0274-8

Bioprinted gelatin hydrogel platform promotes smooth muscle cell contractile phenotype maintenance

Ajay Tijore[1] · Jean-Marc Behr[1] · Scott Alexander Irvine[1] · Vrushali Baisane[1] · Subbu Venkatraman[1]

Published online: 28 March 2018

Abstract
Three dimensional (3D) bioprinting has been proposed as a method for fabricating tissue engineered small diameter vascular prostheses. This technique not only involves constructing the structural features to obtain a desired pattern but the morphology of the pattern may also be used to influence the behavior of seeded cells. Herein, we 3D bioprinted a gelatin hydrogel microchannel construct to promote and preserve the contractile phenotype of vascular smooth muscle cells (vSMCs), which is crucial for vasoresponsiveness. The microchanneled surface of a gelatin hydrogel facilitated vSMC attachment and an elongated alignment along the microchannel direction. The cells displayed distinct F-actin anisotropy in the direction of the channel. The vSMC contractile phenotype was confirmed by the positive detection of contractile marker gene proteins (α-smooth muscle actin (α-SMA) and smooth muscle-myosin heavy chain (SM-MHC)). Having demonstrated the effectiveness of the hydrogel channels bioprinted on a film, the bioprinting was applied radially to the surface of a 3D tubular construct by integrating a rotating mandrel into the 3D bioprinter. The hydrogel microchannels printed on the 3D tubular vascular construct also orientated the vSMCs and strongly promoted the contractile phenotype. Together, our study demonstrated that microchannels bioprinted using a transglutaminase crosslinked gelatin hydrogel, could successfully promote and preserve vSMC contractile phenotype. Furthermore, the hydrogel bioink could be retained on the surface of a rotating polymer tube to print radial cell guiding channels onto a vascular graft construct.

Keywords 3D extrusion bioprinting · Gelatin hydrogel · Transglutaminase · Vascular prosthesis · Vascular smooth muscle cells · Contractile phenotype

1 Introduction

Currently, synthetic vascular prostheses are used to effectively substitute diseased large diameter blood vessel (>6 mm) (Deutsch et al. 1999; Laube et al. 2000). However, small diameter (<6 mm) synthetic grafts suffer from poor clinical performance and early failure due to thrombosis, and mechanical compliance mismatch with host vasculature (Luscher and Barton 1997; Sayers et al. 1998).

It has been proposed that the performance of a small diameter vascular graft can be improved by the cellularization with vascular cells (endothelial cells and vascular smooth muscle cells (vSMC)) (Baguneid et al. 2006; Lee et al. 2008; Ahn et al. 2015). This is especially relevant in the case of biodegradable constructs that, following implantation, are designed to fully resolve and be replaced by host cells and secreted extracellular matrix (ECM) to give a more natural like tissue. The vSMCs have phenotype plasticity between the proinflammatory secretory and the vasoactive contractile phenotypes. The contractile phenotype is characterized by elongated shape and upregulated contractile proteins expression (α-SMA), and the synthetic phenotype, characterized by increased proliferation, rhomboid morphology and downregulated expression of contractile proteins (Baguneid et al. 2006; Rensen et al. 2007; Campbell and Campbell 2012).

The contractile vSMCs are essential for the vasoresponsiveness of a vessel, in maintaining the blood vessel tone and blood pressure through their contraction and relaxation, hence are desired for a cellularized vascular prosthesis. However, freshly cultured vSMCs initially display a contractile state and after several days of *in vitro* culture adopt the secretory phenotype (Campbell and Campbell 2012; Timraz et al. 2016).

✉ Scott Alexander Irvine
sairvine@ntu.edu.sg

[1] School of Materials Science and Engineering, Nanyang Technological University, 50 Nanyang Avenue, Singapore 639798, Singapore

Cell aligning grooves or channels have been found to promote and preserve the desired contractile phenotype. The vSMCs sense the channel walls or grooves and adapt with orientated elongation in the direction of the features. It has been observed that vSMCs cultured near to confluence on biodegradable film with microchannels from 80 to 300 μm wide became aligned and elongated with enhanced α-SMA expression (Rensen et al. 2007; Shen et al. 2006). Previously, cell aligning scaffolds have frequently been fabricated by indirect methods such as replica molding against a photoresist mold with polydimethylsiloxane (PDMS). This method produced scaffolds with parallel microgrooves (3 μm in width, 5 μm in height), which was capable of trans-differentiating late passage vSMCs with synthetic phenotype into contractile vSMCs (Chang et al. 2014). PDMS is a nonbiodegradable polymer hence its regenerative application is limited. Our group has recently investigated the direct fabrication cell aligning features to influence cell behavior using biodegradable polymers, that following implantation will resolve, allowing host cells to remodel the scaffold to a natural like tissue.

In a previous study, we found meltspun biocompatible and biodegradable polymer polycaprolactone (PCL) could create microchannels by meltspinning that align and preserve the phenotype of contractile vSMC on 2D films and radially around tubes (Agrawal et al. 2015). Subsequently, we found that the same effects were possible by the extrusion printing of PCL on 2D films and tubes (Zhao et al. 2015).

PCL and the related polylactide caprolactone (PLC) have the advantage for use in many scaffolding techniques such as electrospinning, melt spinning and 3D printing, in that it can set instantaneously following dispensing due to thermal setting of the molten polymer or by solvent evaporation (Mondal et al. 2016; Cama et al. 2017). However, both PCL and PLC, being synthetic polymers, lack ECM mimicking properties and cell guidance cues present in protein-based hydrogels (Mondal et al. 2016; Cama et al. 2017).

The 3D bioprinting of protein-based hydrogels have the benefit of ECM like properties and the hydrogels are readily remodeled by host cells. However, the bioprinting of water-soluble hydrogels has the challenge of gelation post-printing and the stabilization of flowable aqueous solutions (Yong He et al. 2016; Merceron and Murphy 2015; Pati et al. 2015). A common approach for the 3D bioprinting of hydrogels is the use of photoinitiated crosslinking of hydrogel monomers. This method has the complication of the chemistry required for the hydrogel monomer modification to support photoinitiated crosslinking (Merceron and Murphy 2015; Pati et al. 2015). We have investigated the use of microbial transglutaminase (mTgase) as a crosslinking agent. This enzyme catalyses the crosslinking between the γ-carbonyl group of glutamine residues and the ε-amino group of a lysine residues (Greenberg et al. 1991; Collighan and Griffin 2009). This makes it suitable as a gelatin hydrogel crosslinking agent since gelatin contains 8.4% glutamine and 2.9% lysine residues (Crescenzi et al. 2002). Previously it was found that the enzyme can be modulated to give a sufficient time window for crosslinking to create a stable 3D printed structure (Irvine et al. 2015). In addition, we have found that hydrogel microchannels bioprinted from mTgase crosslinked gelatin were able to influence cell phenotype and behavior. The printed micochannels were shown to: induce the aligned orientation of human mesenchymal stem cells (hMSCs) and rat neonatal cardiomyocytes; promote myocardial differentiation of the hMSCs cardiomyocyte differentiation; and improve the organization and rate of cardiomyocyte beating (Tijore et al. 2017).

Many hydrogel bioinks can be 3D bioprinted vertically, however, to be able to pattern a tubular graft, the hydrogel must be able to be deliverable onto the surface of a rotating horizontal mandrel. Hence, for this application, the viscosity of the hydrogel must be sufficient to maintain the printed trace and to allow adherence to the rotating mandrel immediately after delivery.

The primary focus of this study was the 3D bioprinting of mTgase crosslinked gelatin to create a vascular graft model that promotes circumferentially-aligned contractile vSMCs, to mimic the alignment in a native blood vessel. We fabricated a microchannel platform by bioprinting mTgase crosslinked gelatin hydrogel to induce and preserve the contractile phenotype of vSMCs. The microchanneled platform improved the cell alignment and distinctly upregulated vSMC contractile markers expression. Furthermore, the observations made on the 2D hydrogel platform were tested for their relevance on a 3D platform by constructing 3D microchanneled tubular vascular graft model to mimic the native blood vessel. For this purpose, hydrogel printing was performed with a 3D bioprinter integrated with a customized rotating mandrel (Fig. 5). The 3D microchanneled vascular construct also enhanced cell alignment while promoting and maintaining vSMC contractile phenotype and downregulating the rate of proliferation.

2 Materials & methods

2.1 Crosslinked gelatin hydrogel substrate fabrication

Gelatin (Bloom 300, type A; Sigma-Aldrich) was dissolved in phosphate buffer saline (PBS) and heated at 60 °C for 2 h to prepare 5% gelatin solution. Then 3 *w/v* % mTgase (TG-BW-MH, 100 U/g, EC 2.3.2.13 with sodium caseinate and maltodextrin additives, Ajinomoto) was then added to the gelatin solution and sterilized with 0.2 μm membrane filter.

To create the foundation of hydrogel film, approximately 100 μl of gelatin mixture was poured onto a polyacetate transparency sheet followed by placing 22 mm glass coverslip on the droplet to spread the hydrogel. Subsequently, the gelatin mixture was placed in an oven at 37 °C overnight to crosslink and then the gelatin-coated coverslips were detached from the sheet.

2.2 3D bioprinting of gelatin hydrogel

For gelatin bioprinting, the pressure-controlled robotic dispensing system (Janome 2300 N) was employed. The printing coordinates were programmed using JR-C point software (supplied by the manufacturer) (Irvine et al. 2015; Bhuthalingam et al. 2016). The hydrogel dispensing pressure and robot arm speed were set to 0.1 MPa and 10 mm/s respectively. The mTgase/ 5% Gelatin solution was printed onto the gelatin-coated coverslips using syringe equipped with 30-gauge needle (inner diameter 160 μm). Further, gelatin printed substrates were allowed to crosslink overnight in an oven at 37 °C (Irvine et al. 2015).

2.3 Gelatin hydrogel characterization

The gelatin hydrogel mass loss and swelling ratio were assessed to calculate the hydrogel's degradation and water-bearing capacity respectively (Vatankhah et al. 2014). For that, gelatin hydrogel substrates ($n = 3$) were submerged in smooth muscle cell complete medium and placed in the incubator at 37 °C for 7, 14 and 21 days. Gelatin hydrogel substrates were initially weighed before immersing in the medium (W). During the incubation period, the culture media was replaced every 3 days. After a specified time interval, substrates were removed from the medium, weighed (W_0) and vacuum dried. Furthermore, vacuum dried substrates were weighed to assess their weights (W_d). The percent mass loss (degradation) and swelling ratio of gelatin hydrogel substrates were calculated by using following formula.

$$\text{Mass loss } (\%) : (W - W_d)/W \times 100$$
$$\text{Swelling ratio } (\%) : \ W_0 - W_d/W_d \times 100$$

2.4 Polylactide caprolactone small diameter vascular graft model fabrication by dip coating.

Stainless steel rods (4 mm diameter) were attached to a homogenizer and dipped into a glass cylinder containing polyvinyl alcohol (PVA) solution (15% PVA in 50:50 ethanol and distilled water). The rods were rotated at 300 rpm speed during the dipping to ensure even coating (Puetz and Aegerter 2004). The rods were allowed to rotate for next 5 min and further dried at 60 °C for 30 min. The PLC (monomer feed L:C ratio of 70:30) coat was added by immersing the PVA coated rods in 15% PLC polymer solution in chloroform (also containing 0.6% *w*/w polyethylene glycol (PEG)) at speed of 300 mm/min for immersion and 120 mm/min for withdrawal. After dipping the rods were inverted for 1 min and rotated at 10 rpm for 5 min in the horizontal position.

To release the PLC tube from the mandrel, the polymer coated rods were soaked in water for 48 h to dissolve PVA coating and PEG. After this incubation, the mandrel rod could be easily removed from the PLC tube.

To prepare the PLC 70:30 tubes for gelatin hydrogel printing, the polymer tubes were fitted onto metallic rods and plasma treated. Oxygen plasma treatment was performed on the PLC tubes with a plasma generator consisting of PDC-32G and PDC-FMG Plasmaflo (Harrick Plasma, Ithaca, New York, USA). The tubes were exposed to pure oxygen gas under plasma input power of 100 W for 1 min.

The plasma-treated PLC tube was dip coated with rotation (300 rpm) into a 5% gelatin\mTgase solution. The coated tube was horizontally rotated for 5 mins for a uniform coating then incubated at 37 °C for 30 mins to allow gelatin crosslinking. To print the gelatin microchannels, the 3D bioprinter was modified with the inclusion of a customized programmable mandrel rotator (Fig.5 a,b). The gelatin-coated tube was rotated at 10 rpm during the printing of the hydrogel channels.

2.5 Cell culture

Aortic smooth muscle cells (vSMCs) purchased from (Lonza) cultured in vascular smooth muscle cell growth medium (ATCC) was at 37 °C in humidified atmosphere of 5% CO_2. Hydrogel samples were sterilized with 70% ethanol soaking (1 h) and UV light exposure (30 min). Prior to cell seeding, sterilized samples were equilibrated by soaking in culture media for 24 h. For scaffold seeding, vSMCs were detached from the surface using trypsin/EDTA solution (Invitrogen) and seeded at a concentration of 1×10^5 cells/well of a 6 well plate.

2.6 Cell viability and proliferation assay

Cellular viability and proliferation were assessed using the Alamar blue activated resazurin fluorescence assay (Invitrogen), performed according to the manufacturer's protocol. Briefly, a solution of 10% *v/v* Alamar blue reagent in culture medium was added to the samples (0.25 ml per cm^2 of culture area) and incubated for 1 h at 37 °C. Then, 100 μL of culture medium containing reagent was removed and transferred to a 96 well plate. Spectrophotometric plate reader was utilized to read excitation and emission fluorescence at 560 nm and 585 nm respectively. The cell density was calculated against a pre-prepared standard curve.

2.7 Immunocytochemistry and microscopy

Chemical fixation of cells was done using 4% paraformaldehyde solution for 10 min and then treated with 0.1% Triton X-100 for 5 min. The samples were blocked with 5% bovine serum albumin (BSA) and incubated with primary mouse monoclonal anti α-smooth muscle actin IgG (1:200, Sigma) or rabbit polyclonal anti-smooth muscle myosin heavy chain IgG (1:50, Abcam) for 1 h at 37 °C. The samples were washed

thrice with PBS and further labeled with the secondary Alexa Fluor 488 goat anti-mouse IgG (1:200, Invitrogen) or Alexa Fluor 568 goat anti-rabbit IgG (1:100, Invitrogen). Rhodamine-phalloidin dye (1:400, Invitrogen) was used for F-actin staining. Cell nuclei were stained with 4′-6-diamidino-2-phenylindole (DAPI) (Invitrogen). Calcein AM dye solution (1:500) was used for live cell imaging purpose. Fluorescent images were taken with an Eclipse 80i upright microscope (Nikon). Images of vSMC morphology, as well as gelatin microchannel features, were observed and recorded using optical microscopy (Nikon Eclipse TS100).

2.8 Image analysis and statistical study

F-actin stained cell images were assessed to quantify the F-actin stress fibre orientation (McCloy et al. 2014; Bolte and Cordelieres 2006). The OrientationJ[19] plugin of ImageJ Software was employed to process F-actin stained images and to construct the hue-saturation-brightness (HSB) color-coded map of F-actin stress fibre orientation. A histogram was generated by using the stress fibre orientation values of at least 10 individual images from each group. The aspect ratio of a cell is the indicator of the degree of the cell of elongated morphology and is calculated by dividing the cell length by cell width using the 'Measure' function of ImageJ software.

The corrected total cell fluorescence (CTCF) for α-SMA staining was calculated using ImageJ. In brief, the cell area was outlined and the cell area and mean fluorescence were computed with background adjustment. CTCF was calculated using following formula, CTCF = integrated density – (area of selected cell × mean fluorescence of background readings) (McCloy et al. 2014). The α-SMA and F-actin co-localization were evaluated by analyzing the Mander's colocalization coefficient using the JACoP plugin installed in ImageJ (Bolte and Cordelieres 2006). Mander's colocalization coefficient here estimates the co-distribution of α-SMA fluorescence intensity with F-actin fluorescence intensity (Bolte and Cordelieres 2006).

Student t-test was used to determine the statistical significance. Sample size data is mentioned in the corresponding figure legends. Error bar represents mean value ± standard deviation.

3 Results

3.1 Swelling and stability of bioprinted hydrogel microchannels

A previously established method of crosslinked gelatin hydrogel preparation was implemented in this study (Irvine et al. 2015). For the bioprinted scaffold fabrication, glass coverslips were uniformly coated with gelatin hydrogel solution and gelatin hydrogel microchannels were printed onto the gelatin film coated coverslips (Fig. 1a). These printed microchannels created the effective spacing of 200 μm at the base (Fig. 1b). The swelling ratio (%) of hydrogel scaffold was evaluated in the presence growth medium for consecutive 3 weeks and it was found in the range of 110% to 120% (Fig. 1c). Furthermore, the hydrogel mass loss (%) was determined to assess the degradation profile of the hydrogels and the results indicated negligible mass loss (2.4%) over a period of 3 weeks (Fig. 1d). These hydrogel characterization studies suggested the development of stable crosslinked hydrogels (Omidian and Park 2010).

3.2 mTgase/gelatin hydrogel microchannel effect on vSMC cell elongation and alignment

The vSMCs were cultured on both the microchannel and the plain hydrogel substrate to evaluate the effect of microchannels on the spatial distribution and morphology of cells. Cell growth was monitored at different time intervals over the span of a week (Fig. 1e). Cells on the microchanneled hydrogel substrate displayed an elongated and well-aligned morphology along the microchannel direction throughout culture duration, while on the plain hydrogel substrate, cells displayed non-aligned and randomly spread morphology which was evident from day 4 of cell culture. To compute the difference in the cell alignment, phalloidin-labeled F-actin stress fibres were analyzed using OrientationJ[19] plugin. HSB color coded maps indicating F-actin stress fibre orientation were generated for the cells from both groups (Fig. 2a & 2b). The stress fibre orientation data clearly illustrated that most of the stress fibres were oriented along microchannels direction as indicated by the histogram (Fig. 2c), whereas, stress fibres of cells grown on the plain hydrogel substrate did not exhibit any unidirectional orientation (Fig. 2d).

The cell aspect ratio was also quantified to check the cell elongation. The higher the aspect ratio, the higher the cell elongation. Patterned vSMCs on the microchanneled substrate showed prominently higher aspect ratio (~8) in comparison to the randomly spread cells (~3) on the plain substrate (Fig. 2e). These results demonstrate that microchanneled hydrogels had a considerable effect in influencing the cellular anisotropy.

3.3 Characterization of microchannel seeded vSMC phenotype

To investigate the effect of microchannel triggered-cellular anisotropy on vSMC phenotype, various vSMC contractile marker genes were assessed. Our immunostaining results ascertained distinct upregulation of contractile phenotype markers (α-SMA and SM-MHC) in the cells grown on microchanneled hydrogel by day 7 (Fig. 3a). In stark contrast, the randomly spread cells on plain hydrogels did not display any prominent expression of contractile phenotype markers, implying a predominantly secretory phenotype. The fluorescence intensity of α-SMA was determined to identify the relative difference between α-SMA

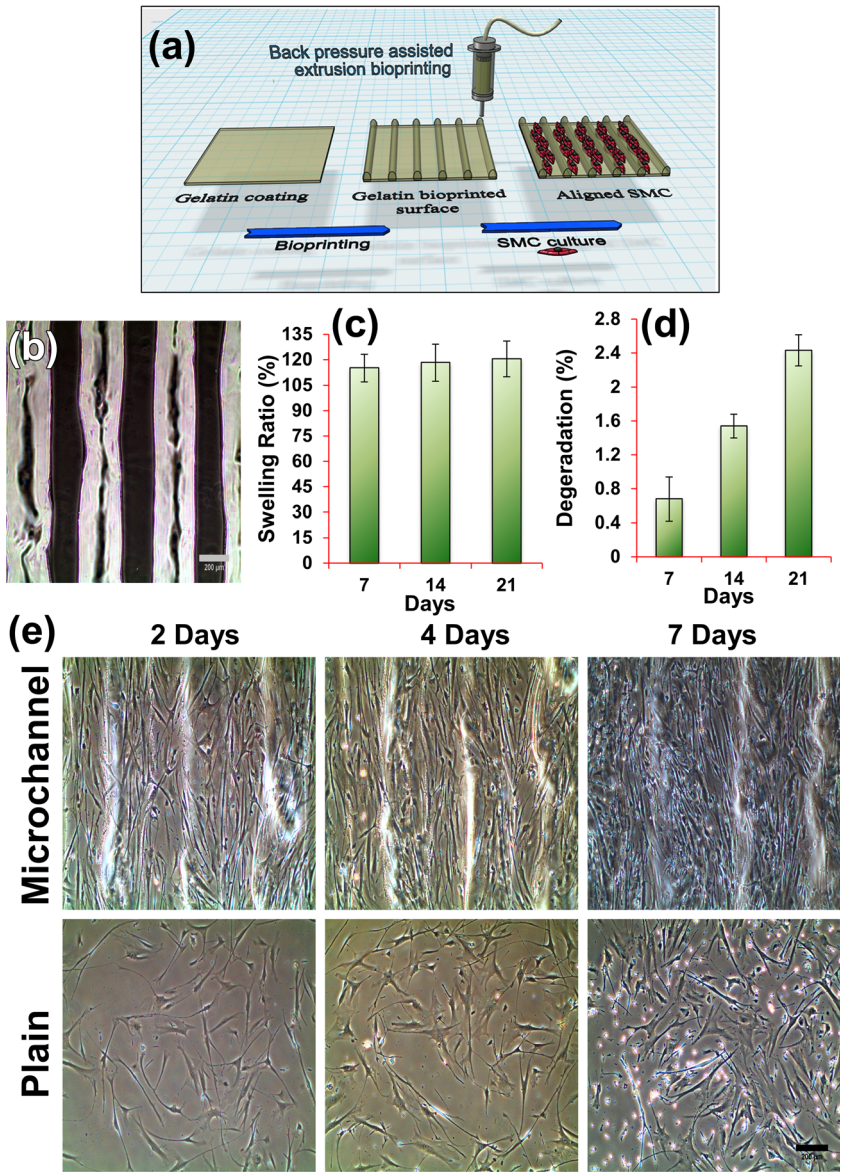

Fig. 1 A schematic illustrating the fabrication of the gelatin hydrogel microchanneled platform (**a**). Microscopic image of the gelatin hydrogel microchanneled surface (**b**). The gelatin hydrogel substrate swelling (**c**) and (**d**) degradation profile in the presence of growth medium were recorded and displayed as histograms. Data represents means ± standard deviation ($n = 3$). Microscopic images of vSMCs grown on microchanneled and plain gelatin substrates demonstrating more elongated and aligned cells on microchanneled substrate (**e**). The scale bar = 200 μm

expression between the groups. Strikingly, microchannel seeded cells displayed a robust increase in α-SMA fluorescence intensity level (eight- to ninefold) than that detected within cells on plain hydrogel (Fig. 3b).

We further observed the incorporation α-SMA into F-actin stress fibre assembly occurring predominantly in the aligned cells on the microchanneled hydrogel (Fig. 4a). However, such colocalization events were markedly downregulated in cells seeded on plain hydrogels. These results are corroborated by previous findings which demonstrated the importance of cellular anisotropy and contractility with the recruitment of α-SMA to F-actin stress fibres (Goffin et al. 2006; Tay et al. 2015). Similarly, α-SMA and stress fibres colocalization index were significantly higher (almost double) for microchannel seeded cells as compared to the unpatterned control (Fig. 4b).

3.4 3D bioprinting of hydrogel microchannels onto a vascular prosthesis model

The final study examined the feasibility of bioprinting mTgase/gelatin microchannels onto a 3D tubular vascular graft model and the effect of the printed channels on seeded vSMCs in this radial context. The hydrogel was printed circumferentially onto the gelatin-coated tubes PLC (70:30 monomer feed ratio) (Fig. 5a,b; Fig. 6a–c). Calcein live cell staining was performed after 7 days to observe the cellular spatial distribution on the vascular construct (Fig. 6d). The calcein-stained images indicated that cells were aligned radially along the microchannel direction on the vascular graft construct. In comparison, cells were randomly spread on the hydrogel coated vascular graft construct. Furthermore, rhodamine phalloidin-stained images also revealed the elongated

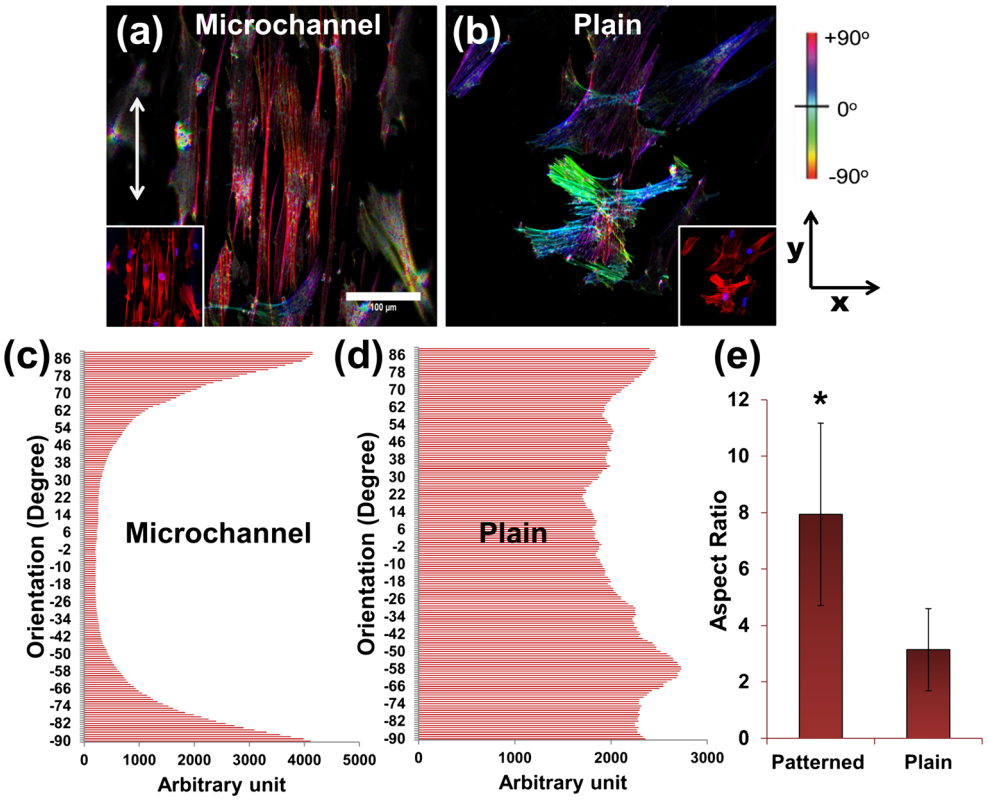

Fig. 2 Microchannel governs F-actin stress fibre orientation. The panel illustrates the hue-saturation-brightness (HSB) color-coded map of F-actin stress fibre orientation for the cells on microchanneled and plain gelatin surface respectively (**a** and **b**). Corresponding histograms of F-actin stress fibre orientation for patterned and unpatterned cells are displayed (**c** and **d**). At least 10 individual images from each group were considered to generate the histograms. Double arrow white line indicates pattern directions. The scale bar = 100 μm. The aspect ratio (indicator of cell elongation) was found to be markedly higher for patterned cells (**e**), data represents means ± s. d., (*$p < 0.05$, $n = 45$)

and aligned arrangement of the cells at the cytoskeletal level (Fig. 6d). In fact, it appears that the aligned vSMCs have formed confluent cell layer across the channels and printed features. As with the bioprinting on the 2D film, it was found that the aligned cells grown on the microchanneled vascular graft model had a distinct expression of α-SMA whereas the non-aligned cells on the unpatterned graft displayed weak α-SMA expression (Fig. 6d).

A cell proliferation assay was performed to assess the effect of the microchannels on vSMC proliferation rates. It was noticed that the rate of proliferation begins to differ significantly between the 2 groups by day 7 and remains so up to day 10 (Fig. 6e).

The observations recorded for the 3D scaffold corroborated the trends identified on the 2D hydrogel platform (i.e. promoting vSMC contractility and its maintenance).

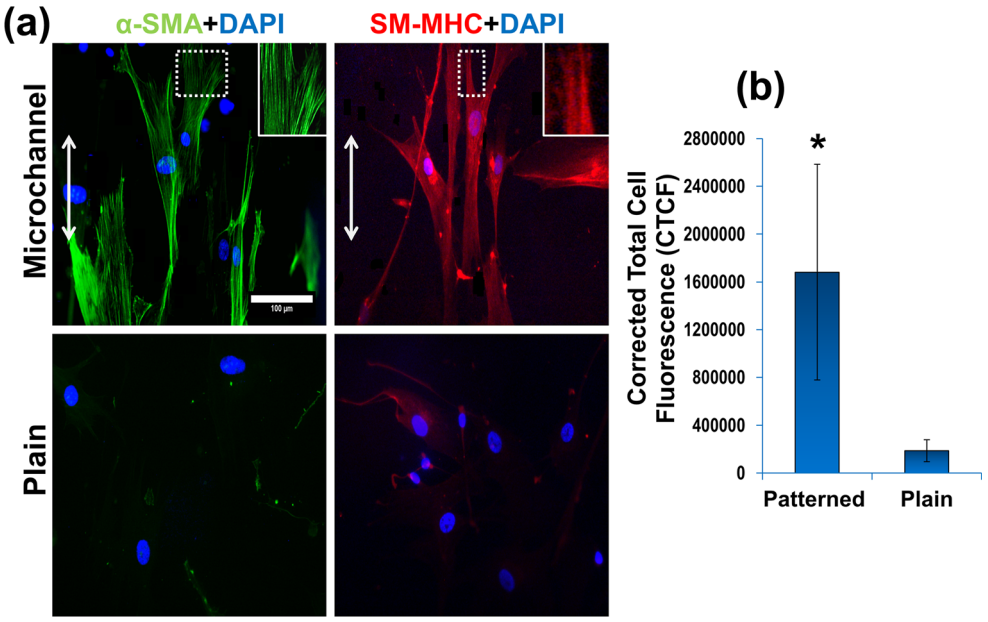

Fig. 3 Microchannel hydrogels promote vSMC contractile marker expression (**a**) vSMCs cultured on microchanneled hydrogels for 7 days displayed prominent expression of α-SMA (green) and SM-MHC (red). Double arrow white line indicates pattern direction. The scale bar = 100 μm. Corrected total cell fluorescence measured using α-SMA green fluorescence intensity was significantly higher for cells on microchanneled surface (**b**), Data represents means ± s. d., (*$p < 0.05$, $n = 21$)

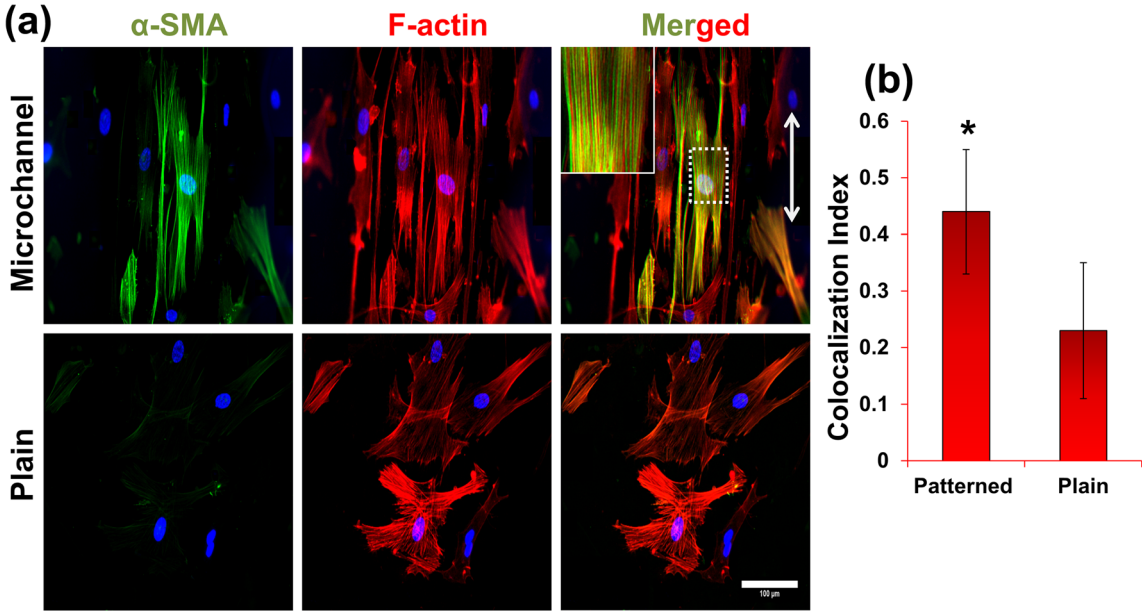

Fig. 4 α-SMA protein incorporation into F-actin stress fibre. Fluorescent images of α-SMA (green), F-actin (red) and DAPI (blue) stained cells from both groups after 7 days (**a**). Double arrow white line indicates pattern direction. The scale bar = 100 μm. (**b**) Colocalization of α-SMA and F-actin fluorescence intensity, data represents means ± s. d., (*$p < 0.05$, $n = 20$). data represents means ± s. d., (*$p < 0.05$, $n = 3$)

4 Discussion

We have previously demonstrated the use of synthetic polymers such as PLC and PCL to create radial vSMC-aligning features on a tubular vascular graft model. Here we show the formation of aqueous hydrogel features by 3D bioprinting for the aligning and phenotype modulation of vSMC.

The choice of a hydrogel polymer for 3D bioprinting depends on the monomer properties. A hydrogel precursor is required to be shear thinning, hence of a flowable viscosity while printing and then become gelled, thus retaining its shape once emerged from the print head. We have found that 5% gelatin (bloom 300) is suitable for such a task. Indeed, this hydrogel precursor can be printed on a turning mandrel without dripping or detachment. The choice of mTgase as a crosslinker also allows the printed trace to adhere to the gelatin coated tube.

The use of gelatin has the additional benefit of producing a highly cytocompatible surface. It has widely been exploited to construct the cell-seeded vascular tissue prosthesis (Ahn et al. 2015; Fu et al. 2014; Zhu et al. 2015). For example, electrospun vascular scaffold, a composite of synthetic polymer and collagen/gelatin were fabricated to facilitate vSMC attachment and growth (Fu et al. 2014). However, the *in vitro* cell seeding of these scaffolds resulted in the growth of randomly spread rhomboid vSMCs characteristic of the synthetic phenotype (Ahn et al. 2015; Fu et al. 2014).

The behavior and phenotype of several cell types have been found to be influenced by surface features (Zhao et al. 2015; Tijore et al. 2015; Abagnale et al. 2015). Such cells have been observed to organize their cytoskeletal elements in the direction of the orientating topography (Prager-Khoutorsky et al. 2011). In our case, F-actin stained images revealed the formation elongated and aligned orientation of stress fibres on both

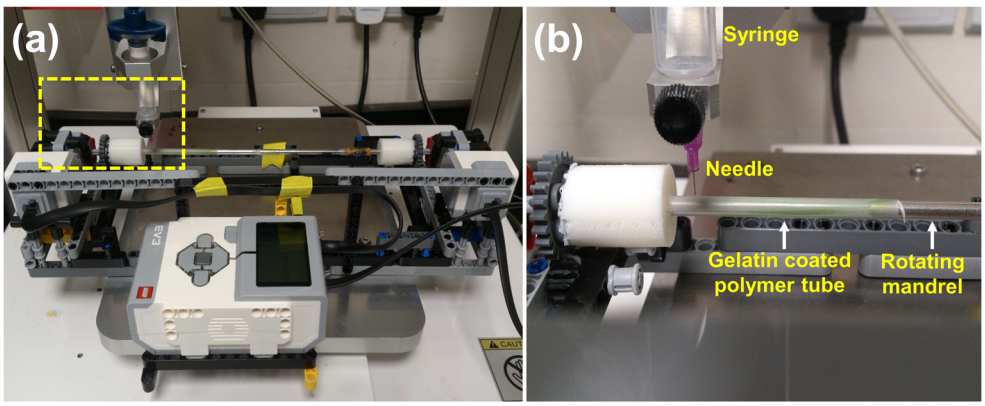

Fig. 5 Addition of a customized rotating mandrel to the bioprinter was used for 3D hydrogel printing with controllable turning speed (**a**). Magnified image displays the close view of polymeric tube mounted on rotating mandrel which is in the close (**b**)

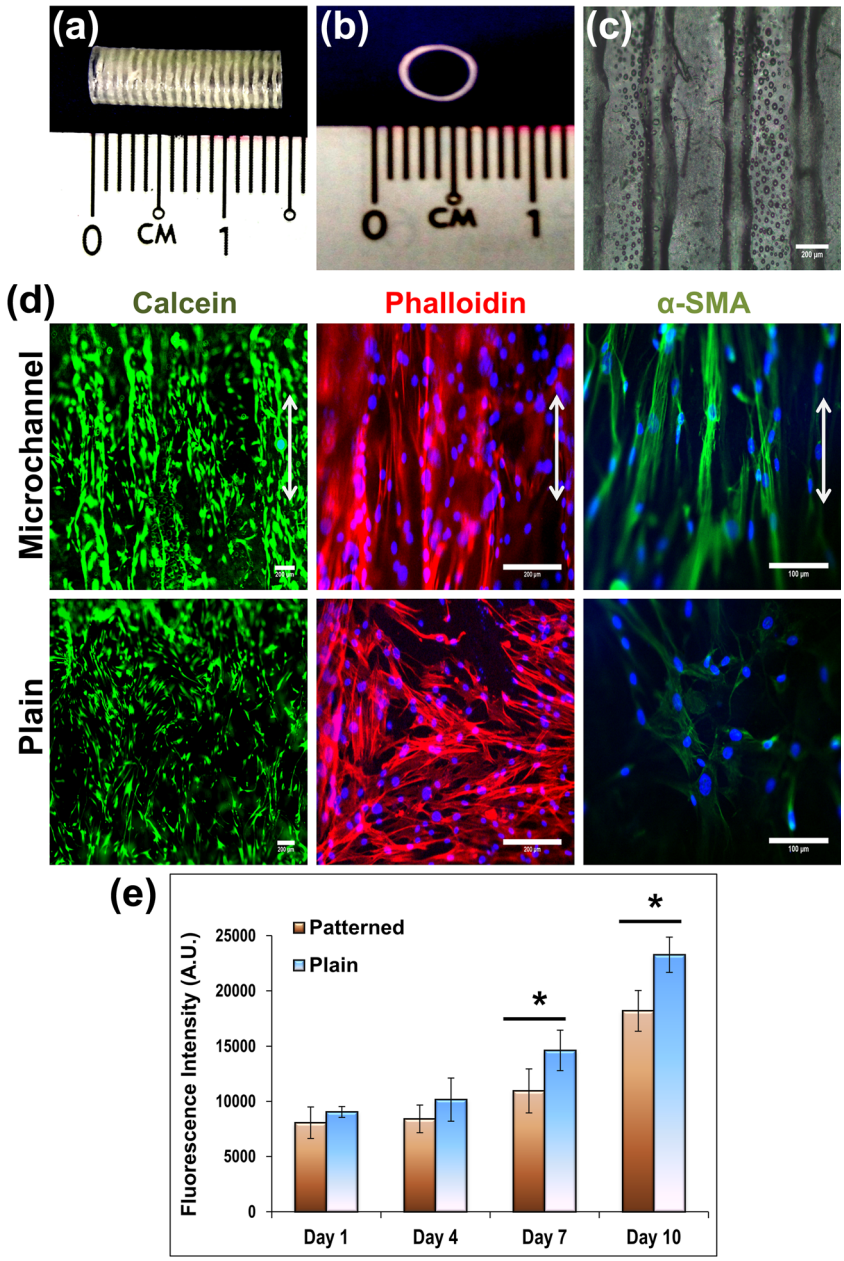

Fig. 6 Fabrication of PLC (70:30) vascular construct and vSMC culture. Gross appearance of the gelatin hydrogel printed and hydrogel-coated PLC 70:30 vascular construct (**a** and **b**). A reprsentative image of the printed hydrogel microchannels on the circumference of the vascular construct was recorded (**c**). The scale bar = 100 μm. Fluorescent images showing calcein-stained cells (green) (**d**), F-actin distribution (red) and α-SMA (green) expression after 7 days of culture. The scale bar is 200 μm (Calcein and F-actin images) and 100 μm (α-SMA images). The cell proliferation was analyzed using Alamar blue assay (**e**). Data represents means ± s. d., (*$p < 0.05$, n = 3)

2D and 3D microchanneled constructs. The spatial distribution of F-actin stress fibres, as shown by the color-coded maps of fibre orientation highlighted their anisotropy with the microchannel directions. Interestingly, the quantification of cellular elongation using the aspect ratio, of the microchannel aligned cells was found to be ~8 which is remarkably near to the aspect ratio of native vSMCs in elastic arteries and differentiated vSMCs (Tay et al. 2015; Rhodin 2011).

It is known that fresh cultures of vSMCs gradually transformed from contractile to synthetic phenotype after several days of *in vitro* culture (Worth et al. 2001). As mentioned, cell aligning topography has been found to preserve the contractile type in culture. Hence, vSMC contractile phenotype evaluation was performed using contractile phenotype gene markers, α-SMA, and SM-MHC. Both markers were detectable for several days of culture on the aligned microchannels confirming the promotion of the contractile phenotype.

Of the marker genes, α-SMA expression is strongly associated with contractile function (Schildmeyer et al. 2000). It was revealed that after 7 days of culture, the cells with microchannel induced-cytoskeletal anisotropy had significantly increased α-SMA incorporation into the actin stress fibres compared to those on the unpatterned surface. It has been found that both the increased α-SMA expression and its incorporation into stress fibers is strongly associated with the differentiation to contractile phenotype for both myofibroblasts and SMCs (Tay et al. 2015; Hinz et al. 2001; Chen et al. 2007).

The final indication of the microchannel aligned vSMCs phenotypic commitment was the clear reduction in their rate of cell proliferation compared to the unpatterned surface seeded cells (Rensen et al. 2007). Interestingly, the mechanism responsible for this growth rate dichotomy in vSMC was found to be through the modulation of the nuclear receptor NOR-1, a transcription factor involved in upregulating synthetic vSMC proliferation (Thakar et al. 2009; Neff et al. 2011; Pashneh-Tala et al. 2015).

The final study demonstrated the transferability of the printed hydrogel guidance from the 2D to the 3D platform by bioprinting the hydrogel microchannels circumferentially on a tubular vascular graft model. The radial aligned contractile vSMC phenotype is desired for a tissue-engineered small diameter blood vessel for their vasoactive properties (Neff et al. 2011; Yazdani et al. 2009; Pashneh-Tala et al. 2015). For this, a customized rotating mandrel was integrated into the 3D printer (Fig. 5). The tubular microchanneled surface provided the topographic guidance to align the cells circumferentially. In addition, the low height of the microchannel walls allowed vSMCs to establish cell-cell contacts all across the scaffold, with aligned cells within channels able to contact those on top of the printed features. Unlike other aligning channels, for which the channel walls are too steep and high to allow cells the cells to connect. (Shen et al. 2006; Cao et al. 2010).

The cells on the unpatterned PLC tube adopted a heterogeneous collection of shapes both rhomboid and elongated. Interestingly in previous studies, vSMCs seeded on a PLC tube without the dip coated layer of gelatin tended to become elongated and aligned longitudinally along the tube rather than radially (Agrawal et al. 2015).

In summary, our 3D microchanneled vascular construct has successfully promoted and preserved vSMC contractile phenotype *in vitro* in order to recreate the functionality of the vasoresponsive vSMC within the medial layer of the native blood vessel.

5 Conclusion

In order to 3D print circumferentially around a tubular vascular prosthesis model, we were able to introduce the modification of a controllable rotating mandrel into the y-axis of a 3D bioprinter.

We optimized and studied the bioprinting of mTgase crosslinked gelatin hydrogel to form a vSMC aligning microchanneled platform, which was found to be applicable to the bioprinting on a 2D film and a 3D tubular vascular construct. In both cases, the hydrogel microchannel promoted and preserved vSMC contractile phenotype to mimic the organization of the native blood vessel. The mTgase crosslinking activity gave sufficient time window for 3D printing a stable hydrogel construct, yet crosslinked the hydrogel without the collapse of the feature. When printing on the rotating the mandrel, the bioink was able to set without displacement or dripping from the rotating tube.

The concept presented here is that a 3D structure can be constructed using 3D printing to instruct vSMCs to adopt a contractile phenotype both on a flat film and circumferentially around a tube. This has relevance for both the tissue engineering of small diameter vascular prosthesis and for the *in vitro* study of contractility of vSMC in a more physiological like arrangement.

Acknowledgements This research is supported by the Singapore National Research Foundation under CREATE programme (NRF-Technion): The Regenerative Medicine Initiative in Cardiac Restoration Therapy Research Program.

Compliance with ethical standards

Statement of ethical approval No ethical approval was required for this study.

Conflict of interest The authors declare no conflict of interests.

References

G. Abagnale, M. Steger, V.H. Nguyen, N. Hersch, A. Sechi, S. Joussen, B. Denecke, R. Merkel, B. Hoffmann, A. Dreser, U. Schnakenberg, A. Gillner, W. Wagner, Surface topography enhances differentiation of mesenchymal stem cells towards osteogenic and adipogenic lineages. Biomaterials **61**, 316–326 (2015)

A. Agrawal, B.H. Lee, S.A. Irvine, J. An, R. Bhuthalingam, V. Singh, K.Y. Low, C.K. Chua, S.S. Venkatraman, Smooth muscle cell alignment and phenotype control by melt spun Polycaprolactone fibers for seeding of tissue engineered blood vessels. Int. J. Biomater. 434876 (2015)

H. Ahn, Y.M. Ju, H. Takahashi, D.F. Williams, J.J. Yoo, S.J. Lee, T. Okano, A. Atala, Engineered small diameter vascular grafts by combining cell sheet engineering and electrospinning technology. Acta Biomater. **16**, 14–22 (2015)

M.S. Baguneid, A.M. Seifalian, H.J. Salacinski, D. Murray, G. Hamilton, M.G. Walker, Tissue engineering of blood vessels. Br. J. Surg. **93**, 282–290 (2006)

R. Bhuthalingam, P.Q. Lim, S.A. Irvine, and S.S. Venkatraman, Automated Robotic Dispensing Technique for Surface Guidance and Bioprinting of Cells, J. Vis. Exp. **117**, e54604 (2016)

S. Bolte, F.P. Cordelieres, A guided tour into subcellular colocalization analysis in light microscopy. J. Microsc. **224**, 213–232 (2006)

G. Cama, D.E. Mogosanu, A. Houben and P. Dubruel, Synthetic biodegradable medical polyesters: Poly-ε-caprolactone. In Xiang Zhang (Ed.), *Science and Principles of Biodegradable and Bioresorbable Medical Polymers* (Woodhead Publishing, 2017)

J.H. Campbell, G.R. Campbell, Smooth muscle phenotypic modulation–a personal experience. Arterioscler. Thromb. Vasc. Biol. **32**, 1784–1789 (2012)

Y. Cao, Y.F. Poon, J. Feng, S. Rayatpisheh, V. Chan, M.B. Chan-Park, Regulating orientation and phenotype of primary vascular smooth muscle cells by biodegradable films patterned with arrays of microchannels and discontinuous microwalls. Biomaterials **31**, 6228–6238 (2010)

S. Chang, S. Song, J. Lee, J. Yoon, J. Park, S. Choi, J.K. Park, K. Choi, C. Choi, Phenotypic modulation of primary vascular smooth muscle cells by short-term culture on micropatterned substrate. PLoS One **9**, e88089 (2014)

J. Chen, H. Li, N. SundarRaj, J.H. Wang, Alpha-smooth muscle actin expression enhances cell traction force. Cell Motil. Cytoskeleton **64**, 248–257 (2007)

C.Y. Tay, Y-L. Wu, P. Cai, N.S. Tan, S.S Venkatraman, X. Chen, L.P Tan, Bio-inspired micropatterned hydrogel to direct and deconstruct hierarchical processing of geometry-force signals by human mesenchymal stem cells during smooth muscle cell differentiation. NPG Asia Materials **7**, e199 (2015)

R.J. Collighan, M. Griffin, Transglutaminase 2 cross-linking of matrix proteins: Biological significance and medical applications. Amino Acids **36**, 659–670 (2009)

V. Crescenzi, A. Francescangeli, A. Taglienti, New gelatin-based hydrogels via enzymatic networking. Biomacromolecules **3**, 1384–1391 (2002)

M. Deutsch, J. Meinhart, T. Fischlein, P. Preiss, P. Zilla, Clinical autologous *in vitro* endothelialization of infrainguinal ePTFE grafts in 100 patients: A 9-year experience. Surgery **126**, 847–855 (1999)

W. Fu, Z. Liu, B. Feng, R. Hu, X. He, H. Wang, M. Yin, H. Huang, H. Zhang, W. Wang, Electrospun gelatin/PCL and collagen/PLCL scaffolds for vascular tissue engineering. Int. J. Nanomedicine **9**, 2335–2344 (2014)

J.M. Goffin, P. Pittet, G. Csucs, J.W. Lussi, J.J. Meister, B. Hinz, Focal adhesion size controls tension-dependent recruitment of alpha-smooth muscle actin to stress fibers. J. Cell Biol. **172**, 259–268 (2006)

C.S. Greenberg, P.J. Birckbichler, R.H. Rice, Transglutaminases: Multifunctional cross-linking enzymes that stabilize tissues. FASEB J. **5**, 3071–3077 (1991)

B. Hinz, G. Celetta, J.J. Tomasek, G. Gabbiani, C. Chaponnier, Alpha-smooth muscle actin expression upregulates fibroblast contractile activity. Mol. Biol. Cell **12**, 2730–2741 (2001)

S.A. Irvine, A. Agrawal, B.H. Lee, H.Y. Chua, K.Y. Low, B.C. Lau, M. Machluf, S. Venkatraman, Printing cell-laden gelatin constructs by free-form fabrication and enzymatic protein crosslinking. Biomed. Microdevices **17**, 16 (2015)

H.R. Laube, J. Duwe, W. Rutsch, W. Konertz, Clinical experience with autologous endothelial cell-seeded polytetrafluoroethylene coronary artery bypass grafts. J. Thorac. Cardiovasc. Surg. **120**, 134–141 (2000)

S.J. Lee, J. Liu, S.H. Oh, S. Soker, A. Atala, J.J. Yoo, Development of a composite vascular scaffolding system that withstands physiological vascular conditions. Biomaterials **29**, 2891–2898 (2008)

T.F. Luscher, M. Barton, 'Biology of the endothelium. *Clin. Cardiol.* **20**, II-3-10 (1997)

R.A. McCloy, S. Rogers, C.E. Caldon, T. Lorca, A. Castro, A. Burgess, Partial inhibition of Cdk1 in G 2 phase overrides the SAC and decouples mitotic events. Cell Cycle **13**, 1400–1412 (2014)

T.K. Merceron, S.V. Murphy, in *Anthony Atala and James J. Yoo (Eds.), Essentials of 3D Biofabrication and Translation*. Hydrogels for 3D Bioprinting applications (Academic Press, Boston, 2015)

D. Mondal, M. Griffith, S.S. Venkatraman, Polycaprolactone-based biomaterials for tissue engineering and drug delivery: Current scenario and challenges. Int. J. Polym. Mater. Polym. Biomater. **65**, 10 (2016)

L.P. Neff, B.W. Tillman, S.K. Yazdani, M.A. Machingal, J.J. Yoo, S. Soker, B.W. Bernish, R.L. Geary, G.J. Christ, Vascular smooth muscle enhances functionality of tissue-engineered blood vessels *in vivo*. J. Vasc. Surg. **53**, 426–434 (2011)

H. Omidian, K. Park, Introduction to hydrogels. in, *Biomedical applications of hydrogels handbook* (Springer, 2010)

S. Pashneh-Tala, S. MacNeil, F. Claeyssens, *The Tissue-Engineered Vascular Graft-Past, Present, and Future* (B Rev, Tissue Eng Part, 2015)

F. Pati, J. Jang, W.L. J.W. Lee, D.W. Cho, Extrusion Bioprinting. In Anthony Atala and James J. Yoo (Eds.), Essentials of 3D Biofabrication and Translation (Academic Press, 2015)

M. Prager-Khoutorsky, A. Lichtenstein, R. Krishnan, K. Rajendran, A. Mayo, Z. Kam, B. Geiger, A.D. Bershadsky, Fibroblast polarization is a matrix-rigidity-dependent process controlled by focal adhesion mechanosensing. Nat. Cell Biol. **13**, 1457–1465 (2011)

J. Puetz, M. A. Aegerter, Dip Coating Technique. in Michel A. Aegerter and Martin Mennig (eds.), *Sol-Gel Technologies for Glass Producers and Users* (Springer US: Boston, MA, 2004)

S.S. Rensen, P.A. Doevendans, G.J. van Eys, Regulation and characteristics of vascular smooth muscle cell phenotypic diversity. Neth. Heart J. **15**, 100–108 (2007)

J.A.G. Rhodin, Architecture of the Vessel Wall. In, *Comprehensive Physiology* (John Wiley & Sons, Inc., 2011)

R.D. Sayers, S. Raptis, M. Berce, J.H. Miller, Long-term results of femorotibial bypass with vein or polytetrafluoroethylene. Br. J. Surg. **85**, 934–938 (1998)

L.A. Schildmeyer, R. Braun, G. Taffet, M. Debiasi, A.E. Burns, A. Bradley, R.J. Schwartz, Impaired vascular contractility and blood pressure homeostasis in the smooth muscle alpha-actin null mouse. FASEB J. **14**, 2213–2220 (2000)

J.Y. Shen, M.B. Chan-Park, B. He, A.P. Zhu, X. Zhu, R.W. Beuerman, E.B. Yang, W. Chen, V. Chan, Three-dimensional microchannels in biodegradable polymeric films for control orientation and phenotype of vascular smooth muscle cells. Tissue Eng. **12**, 2229–2240 (2006)

R.G. Thakar, Q. Cheng, S. Patel, J. Chu, M. Nasir, D. Liepmann, K. Komvopoulos, S. Li. Cell-shape regulation of smooth muscle cell proliferation. Biophys. J. **96**, 3423–3432 (2009)

A. Tijore, P. Cai, M.H. Nai, L. Zhuyun, W. Yu, C.Y. Tay, C.T. Lim, X. Chen, L.P. Tan, Role of cytoskeletal tension in the induction of Cardiomyogenic differentiation in Micropatterned human mesenchymal stem cell. Adv Healthc Mater **4**, 1399–1407 (2015)

A. Tijore, S. A. Irvine, U. Sarig, P. Mhaisalkar, V. Baisane, S. S. Venkatraman, Contact Guidance for Cardiac Tissue Engineering Using 3D Bioprinted Gelatin Patterned hydrogel, *Biofabrication* **10**(2):025003 (2017)

S.B.H. Timraz, I.A.H. Farhat, G. Alhussein, N. Christoforou, J.C.M. Teo, In-depth evaluation of commercially available human vascular smooth muscle cells phenotype: Implications for vascular tissue engineering. Exp. Cell Res. **343**, 168–176 (2016)

E. Vatankhah, M.P. Prabhakaran, D. Semnani, S. Razavi, M. Morshed, S. Ramakrishna, Electrospun tecophilic/gelatin nanofibers with potential for small diameter blood vessel tissue engineering. Biopolymers **101**, 1165–1180 (2014)

N.F. Worth, B.E. Rolfe, J. Song, G.R. Campbell, Vascular smooth muscle cell phenotypic modulation in culture is associated with reorganisation of contractile and cytoskeletal proteins. Cell Motil. Cytoskeleton **49**, 130–145 (2001)

S.K. Yazdani, B. Watts, M. Machingal, Y.P. Jarajapu, M.E. Van Dyke, G.J. Christ, Smooth muscle cell seeding of decellularized scaffolds: The importance of bioreactor preconditioning to development of a more native architecture for tissue-engineered blood vessels. Tissue Eng. Part A **15**, 827–840 (2009)

Y. He, F.F. Yang, H.M. Zhao, Q. Gao, B. Xia, F. JianZhong, Research on the printability of hydrogels in 3D bioprinting. Sci. Rep. **6**, 29977 (2016)

X. Zhao, S.A. Irvine, A. Agrawal, Y. Cao, P.Q. Lim, S.Y. Tan, S.S. Venkatraman, 3D patterned substrates for bioartificial blood vessels - the effect of hydrogels on aligned cells on a biomaterial surface. Acta Biomater. **26**, 159–168 (2015)

G.C. Zhu, Y.Q. Gu, X. Geng, Z.G. Feng, S.W. Zhang, L. Ye, Z.G. Wang, Experimental study on the construction of small three-dimensional tissue engineered grafts of electrospun poly-epsilon-caprolactone. J. Mater. Sci. Mater. Med. **26**, 112 (2015)